Supporting Information

Detection of molecular binding via charge-induced mechanical response of optical fibers

Yan Guan,[ab] Xiaonan Shan,[ab] Shaopeng Wang,[a] Peiming Zhang,[c] and Nongjian Tao*[a]

[a] Center for Bioelectronics and Biosensors, Biodesign Institute, Arizona State University, Tempe, AZ 85287.
[b] Department of Electrical Engineering, Arizona State University, Tempe, AZ 85287.
[c] Center for Single Molecule Biophysics, Biodesign Institute, Arizona State University, Tempe, AZ 85287.

Geometry of fiber probe

The etched optical fiber probe is considered as a cylindrical shape. Figures S1b and S1c show the distal and upper parts of the fiber. They are of similar diameter which supports the assumption that the etched fiber tip is a cylinder.

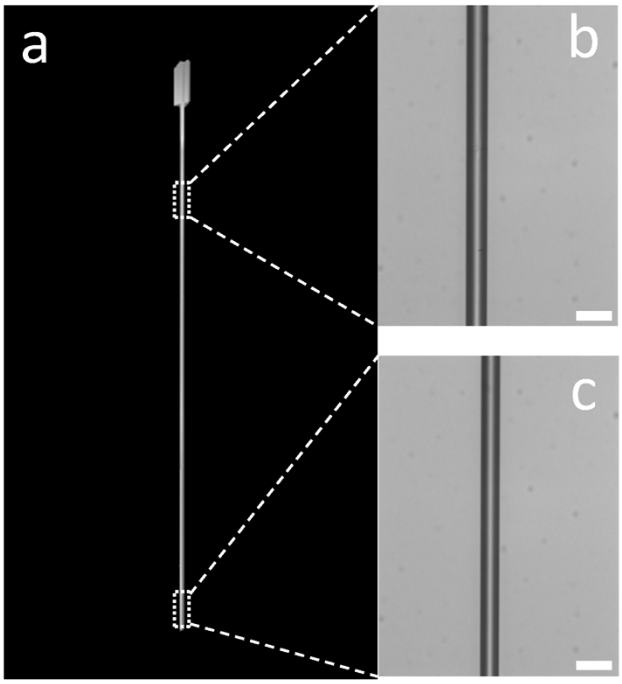

Fig. S1. A typical optical fiber with etched tip viewed from side. (a) Side view of the entire fiber. (b) Zoom in image of the upper part of the fiber. (c) Zoom in image of the lower part of the fiber. Scale bar: 20 µm.

Frequency response of the oscillation amplitude

The oscillation amplitude x_s is given by

$$x_s = \frac{2\pi|E(\vec{\omega})|\sigma r l}{\sqrt{\left(k_{eff} - m_{eff}\omega^2\right)^2 + (c\omega)^2}} \quad , \qquad [S1]$$

where $|E(\vec{\omega})|$ is the electric field strength, k_{eff}, m_{eff}, r and l are the effective spring constant, mass, radius and length of the optical fiber, respectively, and c is the damping coefficient. The effective spring constant, k_{eff}, of the cylindrical optical fiber probe is given by[1]

$$k_{eff} = \frac{3\pi E r^4}{4l^3} \quad , \qquad [S2]$$

where E, r and l are the Young's modulus ,radius and length of the optical fiber, respectively. The electric field strength applied on fiber probe is frequency dependent and given by

$$|E(\vec{\omega})| = \left|\vec{E}_0\right| \frac{R_S}{\sqrt{R_S^2 + \frac{1}{(\omega C_{eff})^2}}} \quad , \qquad [S3]$$

where R_S and C_{eff} are the solution resistance and effective interfacial capacitance respectively. In order to determine the resistance and effective capacitance, we measured the impedance ($|Z(\omega)|$) at different frequencies. $|Z(\omega)|^2$ is given by

$$|Z(\omega)|^2 = R_S^2 + \frac{1}{(\omega C_{eff})^2} \quad . \qquad [S4]$$

By fitting $|Z(\omega)|^2$ and frequency (ω), R_S and C_{eff} can be extracted. Figure S1 shows the fitting of $|Z(\omega)|^2$ and frequency (ω), from which we obtain R_S = 1.68 kΩ, and C_{eff} = 22.11 μF.

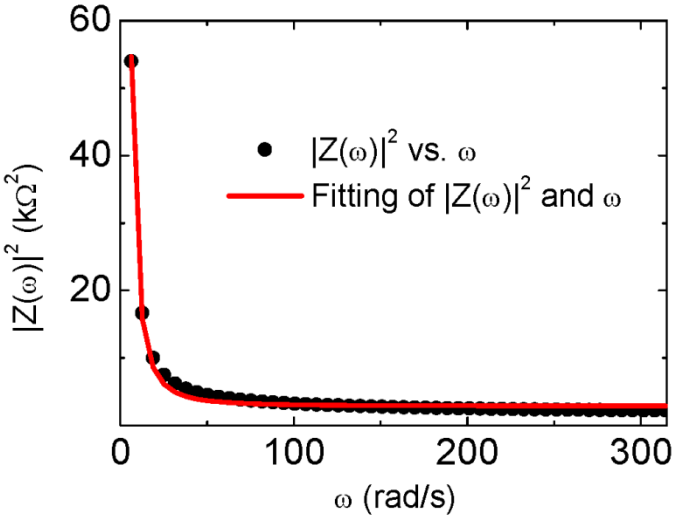

Fig. S2. $|Z(\omega)|^2$ vs. frequency, where the black dots are experimental data, and red line is a fit to Eq. [S4].

From Eqs. **[**S1] and **[**S3], the frequency at which the oscillation amplitude reaches maximum is at

$$\omega_p = \sqrt[4]{\frac{k_{eff}^2}{\left(C_{eff}^2 c^2 - 2k_{eff} m_{eff} C_{eff}^2\right) R_S^2 + m_{eff}^2}} \quad . \qquad [S5]$$

We measured the oscillation amplitude of fiber at different frequencies, from which we determined the maximum frequency, ω_p. Using Eqs. **[**S1] and **[**S3], we fit the oscillation amplitude vs. frequency shown in Figure 2c.

Calibration of oscillation amplitude

The displacement of the optical fiber was determined precisely from the differential optical detection method, which requires calibration. We calibrated the detection method using the following procedure. A region of interest (ROI) including the image of the fiber tip was selected as shown in Figure S2a. The ROI was divided into A and B, marked by red and blue boxes, respectively, and then shifted vertically by different numbers of pixels to mimic the fiber movement (Figure S2*a*). One pixel was determined to be 0.74 μm from the optical system and physical size of CCD camera. The differential intensity at each position was determined from the image. Figure S2b plots the differential intensity vs. pixel position, which shows a linear relation and serves as a calibration curve.

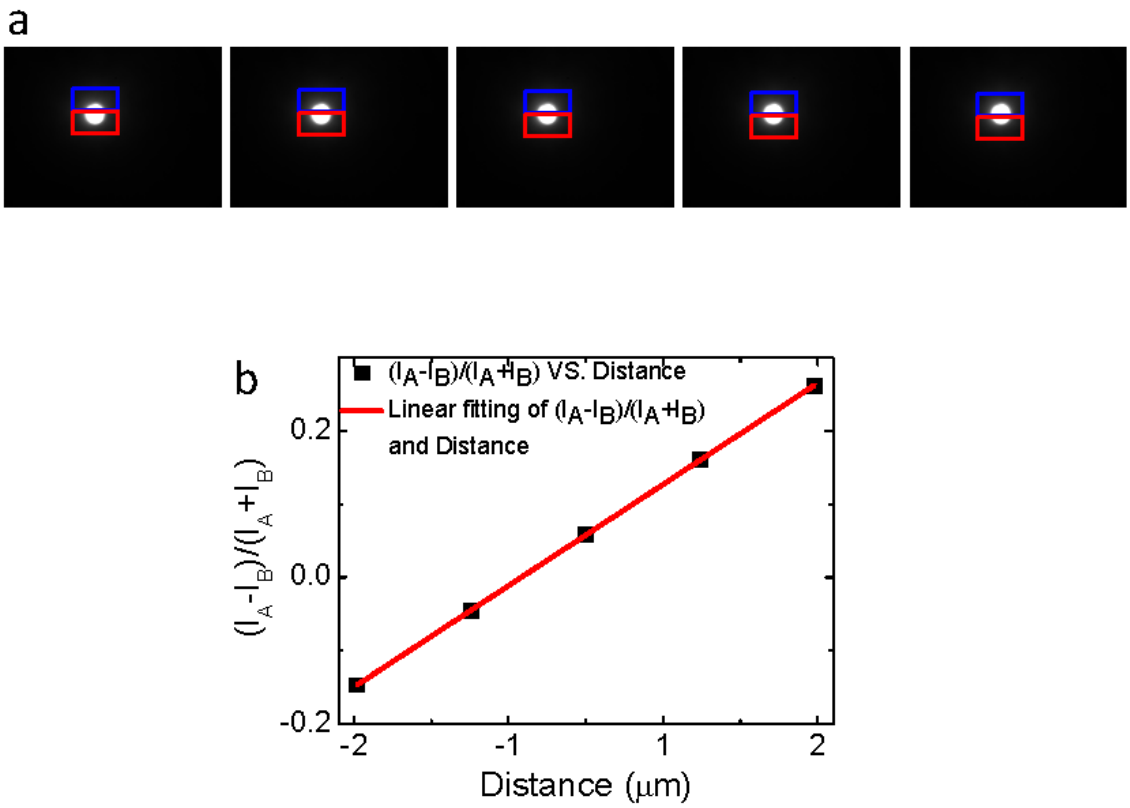

Fig. S3. Calibration of oscillation amplitude. (a) Shifting ROI (red and blue boxes) to mimic fiber movement. From left to right, the ROI is shifted by -2, -1, 0, +1, +2 pixels, where "-" and "+" indicates moving the ROI upward and downward, respectively. (b) Relationship between differential intensity $(I_A-I_B)/(I_A+I_B)$ and fiber movement (shifting of ROI), where the red line is a linear fit to the experimental data (black square).

Ionic screening and effective surface charge density

The surface charge of the optical fiber in aqueous solution is partially screened by counter ions, leading to a reduced surface charge density. The screening factor, defined as the ratio of the effective charge to the actual charge, is calculated as a function of ionic concentration with the Debye-Hückel theory. The screening factor depends on the non-slipping layer thickness (non-slipping layer defines a layer of water that moves with the fiber). The calculation shows that despite the ionic screening substantial effective charge remains even at relative high ionic concentration. For example, ~10% charge remains unscreened at 100 mM of ionic solution.

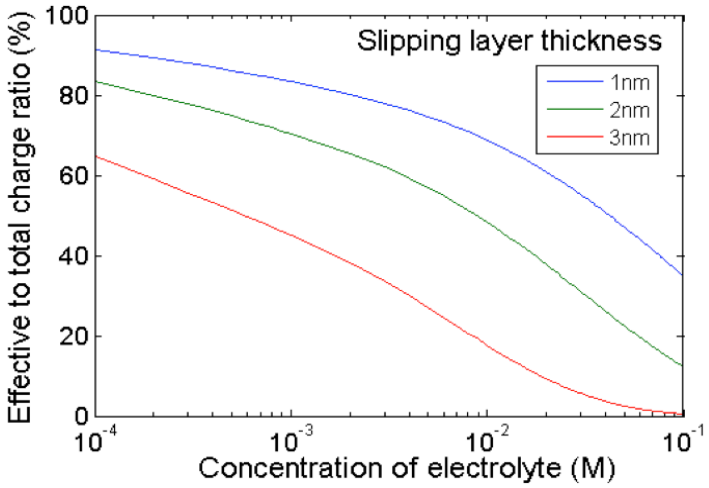

Fig. S4. Ionic screening and effective surface charge density (presented as the ratio of the effective surface charge to the actual charge).

High throughput capability

Fiber bundles

In order to demonstrate high throughput capability, we created an optical fiber bundle consisting of 15 optical fibers manually. Each fiber is 1 cm long with its plastic coating stripped off to expose the silica cladding surface. The fiber bundle was used as a probe and dipped into a well of the 96-well plate containing 0.5 mM NaOH. Figure S4a shows the ends of 9 optical fibers from the bottom of the well through an inverted optical microscope with a 4X objective. Figures S4 b and c show the oscillation displacement and amplitude of the individual fibers over time. The voltage applied was a sinusoidal wave with 20 V of amplitude and frequency of 20 Hz.

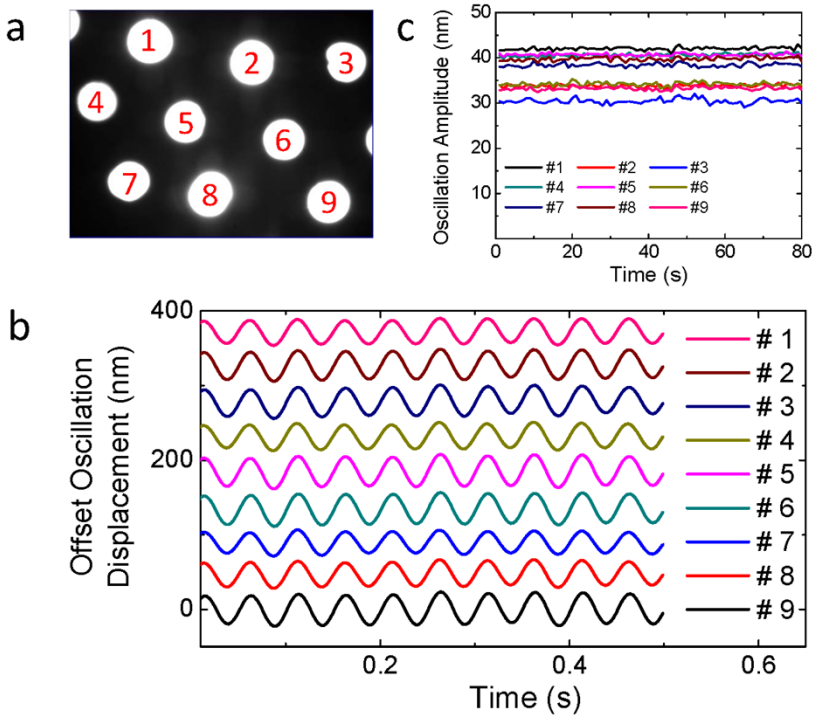

Fig. S5. High throughput detection using an optical fiber bundle (a). Simultaneously measured oscillation displacement (b) amplitude (c) of each fiber over time.

Automated system for multiple well analysis

The microplate consists of 96, 384 and 1536 wells, and each has a unique environment (solution) that is isolated from other wells, allowing for high throughput analysis without cross contamination. An automated control was developed to switch the optical fiber probe from one well to another for high throughput measurement. The control system can be programmed, which moves the optical fiber probe vertically in and out a well, and horizontally from one well to another well for multiple step analysis. The time scale achieved with the setup is 2 s, limited by the motor used in the current setup. Figure S5 shows fast and reproducible amplitude signal as we switched the fiber probe in and out between two solution wells.

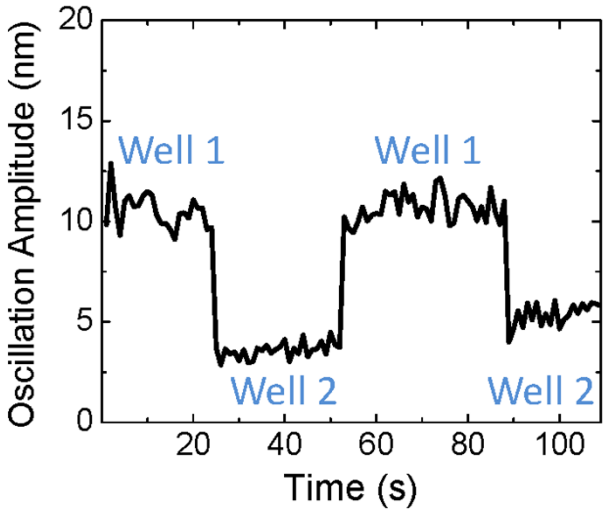

Fig. S6. Automated switching of the optical fiber probe between two wells in a microplate.

Temperature effect

To examine possible temperature effect on the performance, the temperature of solution in the well and the oscillation amplitude of the optical fiber were simultaneously measured. Figure S6a plots the temperature of a solution well within 10 min, which shows ~0.2 °C of temperature drift of the setup. This temperature drift did not cause any detectable changes in the oscillation amplitude of the optical fiber. The buffer solution was heated up to 29 °C and then cooled down. This relative large temperature variation did not produce any detectable drift in the oscillation amplitude either (Figure S6b), which demonstrates excellent temperature stability of the detection platform. However temperature does affect the binding kinetics because of the fundamental thermodynamics of molecular binding processes.

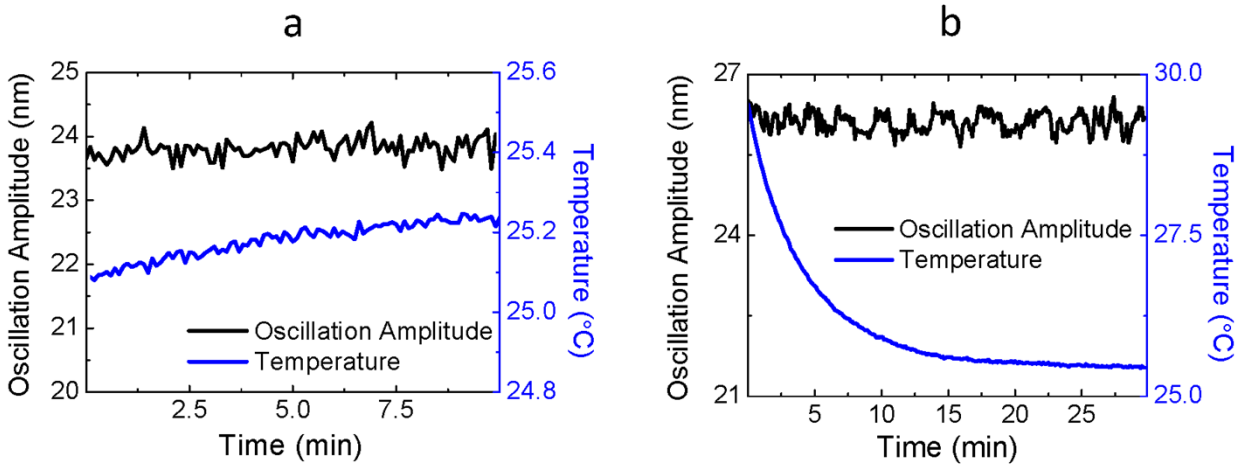

Fig. S7. Temperature Effect. (a) Drift of ambient lab temperature did no affect the fiber oscillation amplitude. (b) Heating and cooling over a large temperature range (4 °C) did not cause a drift in the fiber oscillation amplitude either. Fiber length: 9 mm, diameter: 20 μm. Buffer: 40 times diluted 1XPBS buffer. Vpp = 6 V @ 55 Hz.

Concentration dependence

To demonstrate that the present detection technique can measure different concentrations of analyte, amine-coated optical fibers were modified with BSA via 1, 5-Glutaraldehyde to measure anti-BSA of different concentrations. The fibers were first coated with amine by APTES (see Methods part), and then BSA by incubating them in 2.5% 1, 5-Glutaraldehyde for 15 min and in 0.1 mg/ml BSA for 1 h. Right after the BSA modification, binding of the fibers to different concentrations of anti-BSA were measured and the oscillation amplitude change before and after anti-BSA addition vs. anti-BSA concentration was plotted in Figure S7. The experiment data (dots) were fitted with the Langmuir isotherm, $y = \frac{y_{max} \cdot c}{K_D + c}$, where y, c, and K_D are the oscillation amplitude change, anti-BSA concentration and dissociation constant, respectively. K_D was found to be 2.5 nM from the fitting, which is in agreements with other studies.[2]

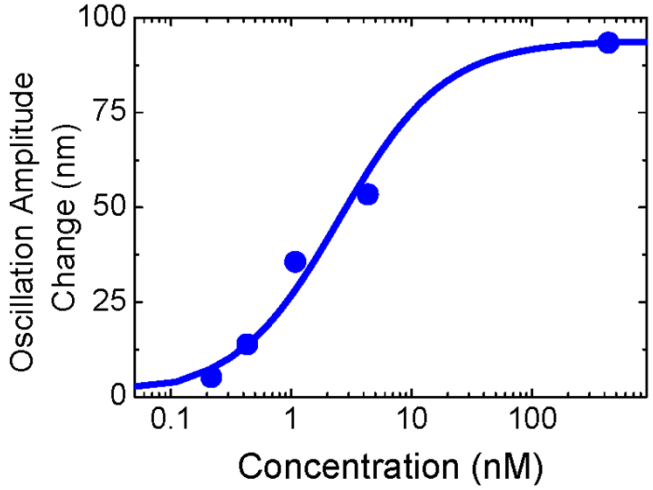

Fig. S8. Response curve of BSA-coated optical fiber to different concentrations of anti-BSA, where the dots are experimental data, and solid line is a best fit of the data to the Langmuir isotherm.

Repeatability

Anti-BSA and BSA

Three optical fibers were prepared following the same procedure (see Experimental Section for details). Briefly, amine coated fibers were incubated in 2.5% 1, 5-Glutaraldehyde for 15 min and then in 0.1 mg/ml BSA for 1 h 15 min. Figure S8 shows the responses of the three optical fibers to 10 µl 0.5 mg/ml anti-BSA (final concentration of 215 nM). The results are similar to each other, demonstrating the repeatability of the present detection technique.

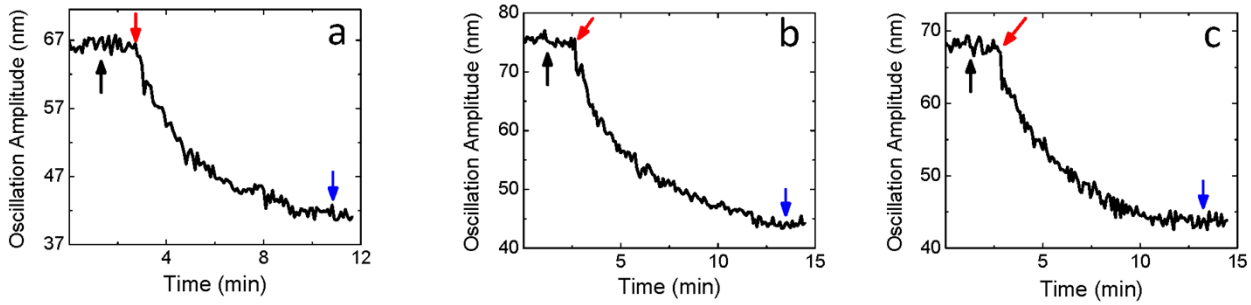

Fig. S9. Measurements anti-BSA binding to BSA with three different optical fibers. The black arrows mark the addition of 10 µl buffer for control, the red arrows mark the additions of 10 µl 0.5 mg/ml anti-BSA (final concentration of 215 nM), and the blue arrows indicate the change of the solution back to buffer. Fiber length: 8.5 mm, diameter: 22 µm. Vpp = 4 V @ 20 Hz.

Imatinib and c-Abl

Figure. S9 shows the binding of imatinib to c-Abl for three different optical fibers. Fibers were modified with c-Abl through 1, 5-Glutaraldehyde according to the procedure described in the Methods part. The responses of the three optical fibers to 10 µl 500 µM imatinib (final concentration of 15 µM) are similar, further demonstrating good reproducibility of the setup.

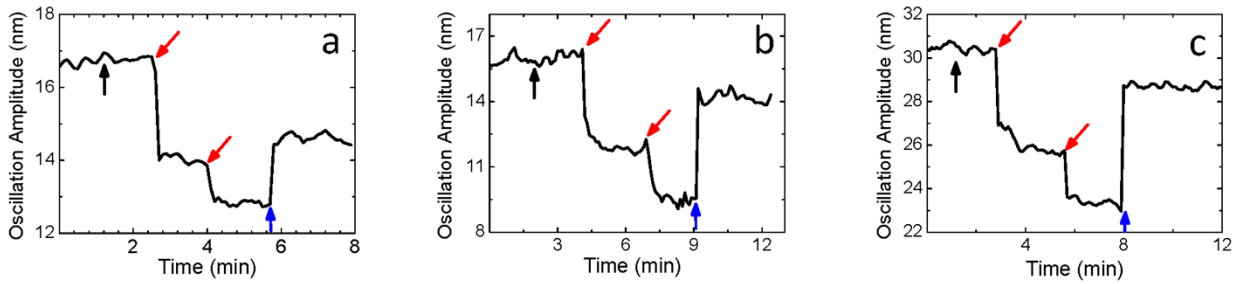

Fig. S10. Measurements of small molecule (imatinib) binding processes with three different optical fibers (*A*, *B* and *C*). These fibers were modified with c-Abl. The black arrows mark the addition of 10 µl buffer, the red arrows mark the additions of 10 µl 500 µM imatinib (final concentration of 15 µM), and the blue arrows indicate the change of the solution back to buffer. Fiber length: (a) 7 mm, (b) 7.5 mm, (c) 7.5 mm. Fiber diameter: (a) 11 µm (b) 13 µm, (c) 12.6 µm. Vpp = 2 V @ 40 Hz.

References

1. S.-H. Chen, H.-N. Lin and P.-M. Ong, *Review of Scientific Instruments*, 2000, **71**, 3788.
2. http://www.biosensingusa.com/downloads/application_note_107.pdf